ELSEVIER

Biomaterials 20 (1999) 475–484

Biomaterials

Preparation of a biphasic porous bioceramic by heating bovine cancellous bone with $Na_4P_2O_7 \cdot 10H_2O$ addition

Feng-Huei Lin[a], Chun-Jen Liao[a], Ko-Shao Chen[b], Jui-Sheng Sun[c,*]

[a] *Institute of Biomedical Engineering, College of Medicine, National Taiwan University, Taipei, Taiwan, ROC*
[b] *Department of Material Engineering, Tatung Technology Institute, Taipei, Taiwan, ROC*
[c] *Department of Orthopaedic Surgery, College of Medicine, National Taiwan University, Taipei, Taiwan, ROC*

Received 2 March 1998; accepted 15 September 1998

Abstract

Sintered bovine cancellous bone exhibited excellent biocompatiblity, high porosity and have an interconnecting porous structure allowing for bone ingrowth. However, the main mineral constitution of sintered bovine bone—hydroxyapatite ($Ca_{10}(PO_4)_6(OH)_2$, HAP) seems to be too stable in vivo. For improving its bioactivity, the calcined bovine bone—removing the organic substance by burning process—with different quantities of sodium pyrophosphate ($Na_4P_2O_7 \cdot 10H_2O$, NP) addition was heated to a high temperature to transform its crystalline phase constitution from HAP into TCP/HAP biphasic or other multiphasic structures. Results revealed that the calcined bovine bone without NP addition, exhibited a pure form of HAP characterized pattern during heating. Its thermal behavior was similar to stoichiometric HAP, it gradually lost its OH^- ions and transformed into oxyhydroxyapatite at high temperature. After being doped into calcined bovine bone, NP would react with HAP to form βTCP and $NaCaPO_4$ around 600°C. At 900°C, doped NP would completely react with HAP and the $NaCaPO_4$ would further react with HAP to form more βTCP in the system. With NP increasing in the calcined bovine bone, HAP would gradually convert into different crystalline phase compositions of TCP/HAP, TCP/HAP/$NaCaPO_4$ or TCP/$NaCaPO_4$ at high temperature. By heating calcined bovine cancellouse bone with different quantities of NP we could obtain different crystalline phase compositions of natural porous bioceramic in this study.

Keywords: Biphasic calcium phosphate; Bioceramic; Xenogeneic bone

1. Introduction

Xenogeneic bone has long been used as a bone grafting material. It is easy to obtain and has lower cost than autogeneic or allogeneic bone graft. However, the clinical application of xenograft has been limited because it involved numerous problems such as infection, disease transfer, and immunological defensive reaction [1, 2]. To overcome these problems, various treatments have been tried with the aim of removing the strongly antigenic proteins and the cellular elements of xenogeneic bone. The Kiel bone splinter, was developed by Martz and Bauermeister et al. [3, 4], using the special maceration process to destroy the protein of bovine bone. Clinically, Kiel bone has been used in orthopedic surgery for filling bone defects [5], but the results of Kiel bone application were still controversial since the deproteination of Kiel bone was incomplete which might have evoked the immuno-defensive reaction [6]. Recently, a pure mineral bone has been developed, removing all organic components of bovine bone and sintering remnant mineral constitution by high-temperature heat-treatment [1, 2]. The sintered cancellous bone maintained the spongy structure of natural bone, which has an interconnecting porous structure, high porosity (about 70 vol%), and a character of osteoconduction allowing for bone ingrowth to form an osseous bed. In comparison to the synthetic porous ceramics, the sintered cancellous bone seems superior to the synthetic porous ceramics. Since the porous calcium phosphate ceramics, using the usual foaming process, has numerous closed pores and bubbly fan walls, the invasion of bone tissue deep into the material would be hampered. Thus, the sintered cancellous

*Corresponding author. Fax: +886 22 394 0049; e-mail: double@ha.mc.nut.edu.tw

0142-9612/99/$ – see front matter
PII: S0142-9612(98)00193-8

bone with an exceptional porous structure has attracted more and more attention in recent years.

The crystalline phase composition of sintered bovine cancellous bone is similar to natural bone mineral—mainly hydroxyapatite ($Ca_{10}(PO_4)_6(OH)_2$, HAP) about 93 wt% and consists of about 7 wt% of β-tricalcium phosphate ($Ca_3(PO_4)_2$, βTCP) [1, 2]. HAP has excellent biocompatiblity, faster bone regeneration, and direct bonding to regenerated bone without intermediate connective tissue [7–9]. However, HAP seems to be too stable in vivo because it shows a similar crystalline phase as bone mineral, which will tend toward chemical and biological equilibrium with bone tissue. βTCP had greater extent dissolution and degradation than those of HAP [9], but some investigators reported that the rate of degradation of βTCP was too fast for optimum bonding to bone [10]. A recent study claimed that the biphasic calcium phosphate (BCP) ceramics, consisting of a mixture of βTCP and HAP, i.e. the weight ratio of 30/70 or 40/60 of βTCP/HAP ceramics, have demonstrated more efficiency in the repair of bone defects than pure HAP or pure βTCP ceramic alone [10–12].

In the study, we tried to develop series of TCP/HAP biphasic calcium phosphates with natural bone structure of interlocking pores that would make physiological fluid deep into the material and provide an osseous bed for bone ingrowth. In our previous study, deficient hydroxyapatite (d-HAP) doped with sodium pyrophosphate ($Na_4P_2O_7 \cdot 10H_2O$, NP) could partially convert d-HAP into βTCP on heating to a temperature up to 600°C. With different NP addition, we could prepare series of TCP/HAP biphasic calcium phosphates in different ratios. Calcined bovine bone was immersed into the NP solution and then heated at an appropriate temperature for sintering and phase transformation. By doping NP into calcined bovine bone (CBB), HAP was partially converted into βTCP at high temperature and TCP/HAP biphasic calcium phosphate bioceramics with a natural bovine bone structure were successfully prepared.

In the present study, we used X-ray diffraction (XRD) analysis to examine the phase transformation of the materials at different heating temperatures. The functional group of CBB and CBB with NP addition at different temperatures were traced by a Fourier-transformed infrared (FTIR) spectroscope. The phase transformation and crystal structure reconstruction of CBB with different NP additions at different heating temperatures were also described in this study.

2. Materials and methods

2.1. Preparation of the specimens

Cancellous bone was obtained from calf femoral condyles and cut into small cubes of approximately 1 cm^3. In order to avoid the cracking and soot formation in the material during the heat-treatment process, the raw bone was boiled in distilled water for 12 h. After boiling, the cancellous bone blocks were dehydrated in an alcohol series and dried at 70°C for 3 days. The dried cancellous bone blocks were calcined at 800°C with a rate of 10°C/min and then maintained for 6 h to remove the organic matrix in a conventional Ni–Cr coiled furnace.

Calcined bovine cancellous bone blocks were soaked in different concentrations of 0.01, 0.02, 0.03, 0.04, 0.05, 0.06, 0.07, 0.08, 0.09, and 0.1 mol/l of $Na_4P_2O_7 \cdot 10H_2O$ solution, respectively, at 70°C for 24 h. Since the surface of the immersed bone blocks contains superfluous immersion solution, a filter paper was used to sop up the redundant NP solution. Then the immersed bone blocks were dried at 70°C for 3 days. The calcined bovine cancellous bone blocks with different quantities of NP additions were sintered, which were placed on the platinum sheet and heated to different temperatures at a rate of 2.5°C/min and maintained for 1 h in a SiC-heated furnace. The materials were cooled to room temperature by slow furnace cooling after heating.

2.2. Evaluation and measurements

The crystalline phases of specimens were determined by the Rigaku X-ray powder diffractometer with CuK_α radiation and Ni filter at the speed of 4°/min. To determine phase contents, relative intensities of the main peaks of each phase were used. The FTIR spectra were recorded using KBr pellets (1 mg sample per 300 mg KBr) on a Jasco FTIR grating instrument with slow scan and normal silt width. The morphology and microstructure of the specimens were observed under the scanning electron microscope (SEM). The surface was coated with a thin layer of carbon of thickness of 2 μm, after being polished with diamond paste and after being etched with 0.1 M HCl for about 10 s. They were then observed by SEM and analyzed using an energy-dispersive electron probe X-ray microanalyzer. P, Ca, and Na were analyzed across the grains and grain boundaries. An electron beam maintained at 2×10^{-10} A was used and X-ray intensities in counts per second (cps) were recorded. The accelerating voltage was 12 kV.

3. Results

3.1. Crystal structure analysis

Figure 1 summarizes the XRD patterns of CBB heating at 1300°C with different NP additions. The CBB without NP addition showed a stoichiometric hydroxyapatite characterized pattern (XRD JCPDS data file No.9-432). As NP addition increased, the intensity of HAP characterized peaks gradually decreased and βTCP

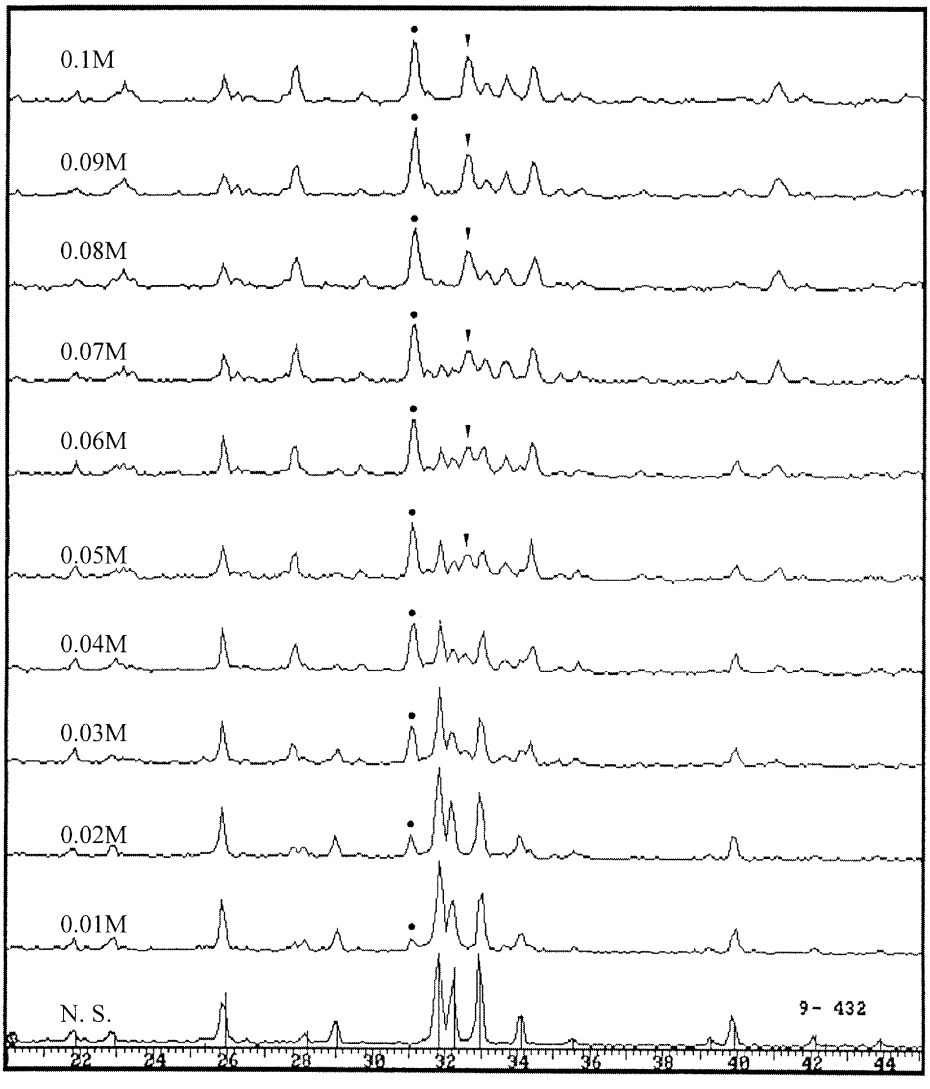

Fig. 1. X-ray diffraction patterns of CBB soaked in different concentrations of NP solution and heated at 1300°C (●: TCP(217); ▼: $NaCaPO_4$ (211)).

characterized peaks appeared progressively. When the concentration of the NP solution is in the range of 0.01–0.04 M, the XRD patterns showed a HAP/TCP biphasic structure where the crystalline phase of CBB was composed by HAP and TCP. Once the concentration of the NP solution is increased to 0.05 M, the rhenanite ($NaCaPO_4$) characterized peaks gradually appear and CBB forms a HAP/TCP/$NaCaPO_4$ multiphasic structure. When the concentration of a NP solution is over 0.08 M, the HAP would completely transform into βTCP where all the characterized peaks of HAP would disappear. Only βTCP and $NaCaPO_4$ characterized peaks existed in the system when the concentration of the NP solution was over 0.08 M (Fig. 1).

To further understand the phase transformation of CBB with NP addition, the CBB with 0.05 M NP addition was prepared and heated at different temperatures. Figures 2 and 3 showed the XRD patterns of CBB and CBB with 0.05 M NP addition, respectively, at different heating temperatures. As shown in Fig. 2, there were no significant differences in XRD patterns of CBB from room temperature to 1300°C where all the characterized peaks of the pattern were in agreement with the HAP XRD JCPDS data file (No. 9-432). After CBB was soaked in 0.05 M NP solution for 24 h and then heated at different temperatures, the intensity of HAP characterized peaks in the pattern showed a negative tendency with heating temperature as shown in Fig. 3. It also shows that the characterized peaks of βTCP and $NaCaPO_4$ start being traced from around 600°C (Fig. 3). As the heating temperature increased, the intensity of the characterized peaks for βTCP and $NaCaPO_4$ gradually increased. As

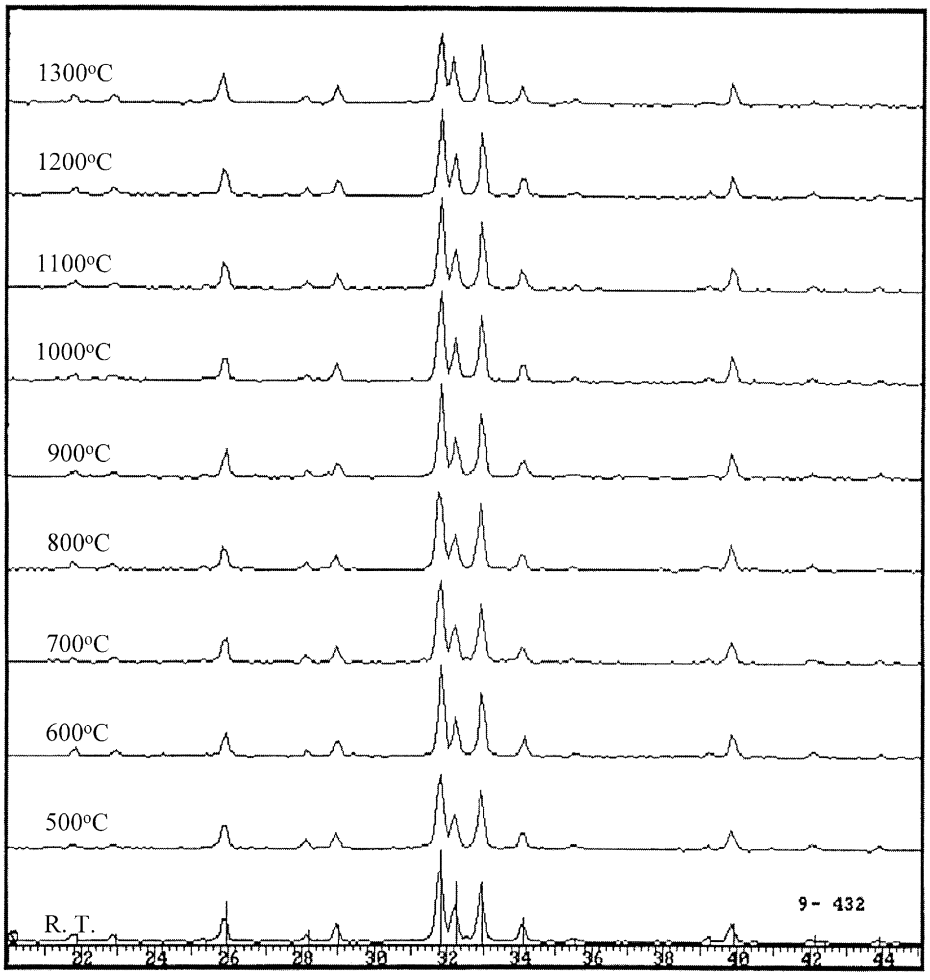

Fig. 2. X-ray diffraction patterns of CBB heated from room temperature to 1300°C.

the heating temperature is increased 1000°C, the intensity of βTCP characterized peaks still increases with heating temperature but the intensity of $NaCaPO_4$ characterized peaks gradually decrease.

3.2. FTIR spectra analysis

The FTIR spectra of CBB heated at different temperatures are shown in Fig. 4. There are no significant differences in the FTIR spectra of CBB from room temperature to 900°C. As the heating temperature is increased to 1000°C, the band of OH^- at 635 cm^{-1} gradually decreases in its intensity with increasing temperature and it disappears at around 1300°C. The FTIR spectra of CBB with 0.05 M NP addition heated from room temperature to 1300°C are shown in Fig. 5. The bands at 1185, 925 and 720 cm^{-1} correspond to the NP functional group and the other bands belong to the HAP structure. The intensity of NP bands gradually decreased as the heating temperature is increased to 500°C and then disappeared around 900°C. The OH^- band of HAP also gradually decreased in its intensity while the heating temperature is increased to 800°C. The bands at 1118 and 945 cm^{-1} corresponding to TCP were observed around 800°C. The TCP bands appeared significantly at 1118, 973, 945, 603, 586, 649 and 540 cm^{-1} when the heating temperature is over 1100°C.

3.3. Microstructure and NP addition

Figure 6a shows the SEM observation of the fracture surfaces of the bovine cancellous bone block after heating at 800°C. Its surface and interior structure contains numerous interconnecting micropores. When the CBB block was soaked into NP solution, it would like a sponge absorb NP into the material uniformly (as seen in Fig. 6b). After being immersed in different concentrations of NP solution for 24 h, the CBB increased in

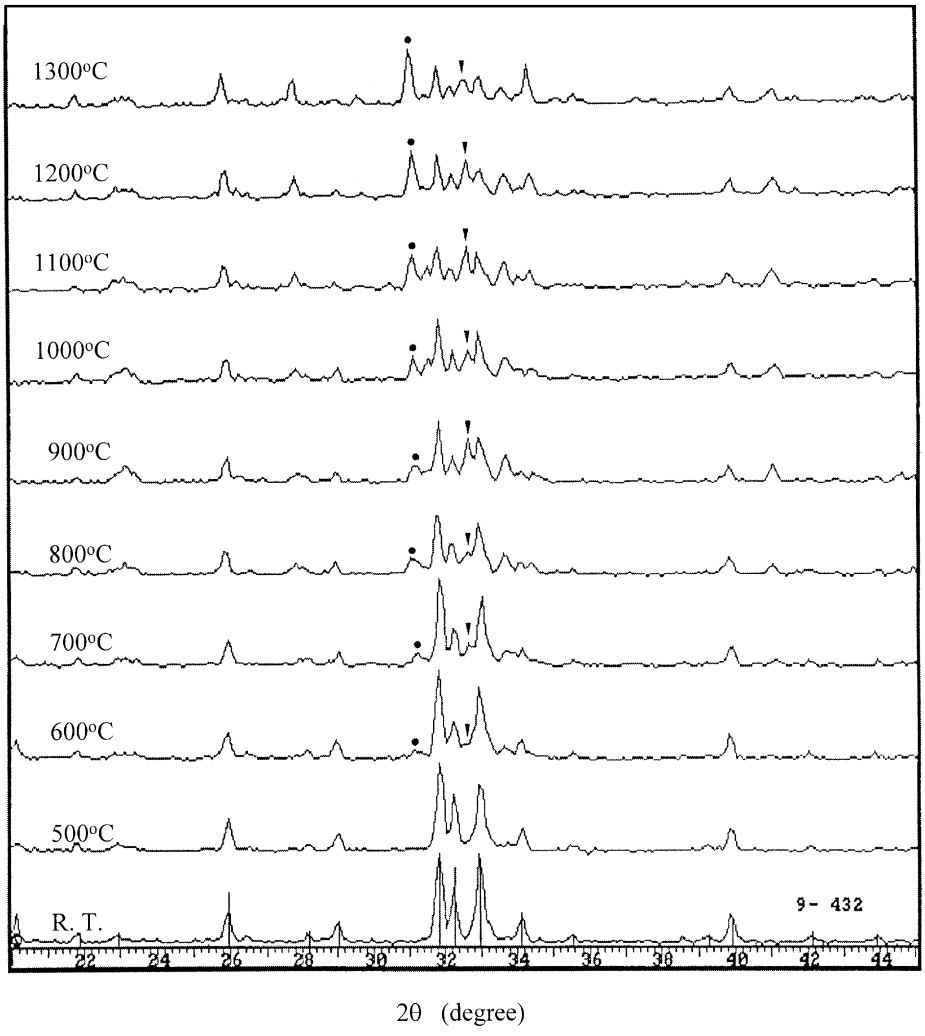

Fig. 3. X-ray diffraction patterns of CBB soaked in 0.05 M NP solution and heated from room temperature to 1300°C (●: TCP(217); ▼: $NaCaPO_4$ (211)).

weight which was in terms of the content of NP in CBB. It showed that NP in CBB increases with the concentration of NP solution as shown in Fig. 7.

Figure 8 shows the SEM micrograph of the CBB with 0.03 M NP addition after heating at 1300°C. Although the CBB has converted its crystalline constitution from pure HAP into TCP/HAP biphasic structure, it could also maintain the spongy structure of natural cancellous bone. As seen in its interior microstructure (Fig. 9a), the material was well-sintered and some of the original bony structures such as Haversian system, Volkmann's canals and lacunae could also be preserved. On etching with o.1 M HCl solution, the sintered biphasic ceramic exhibited a polycrystalline structure with small grain size of about 1–2 μm on average (Fig. 9b). Figure 10 shows the SEM microstructure of the trabecular section of CBB with 0.09 M NP addition after being heated at 1300°C. It also shows a polycrystalline structure after being etched with 0.1 M HCl, where two types of grain-shaped dendrites and granules could be clearly observed in the SEM micrographs of Fig. 10a and b, respectively. The dendrite was identified as $NaCaPO_4$ by EPMA analysis and the granule was supposed to be βTCP. The dentrite crystals were uniformly dispersed in TCP granules.

4. Discussion

In recent years, as a means of improving the biocompatibility of metal materials in vivo, coating HAP onto the metal implant surface using the plasma-spraying technique has been widely investigated [13–15]. To deposit HAP on a metal surface one should introduce HAP powder into a high-temperature flame, therefore, the thermal behavior of HAP has been gradually attracting

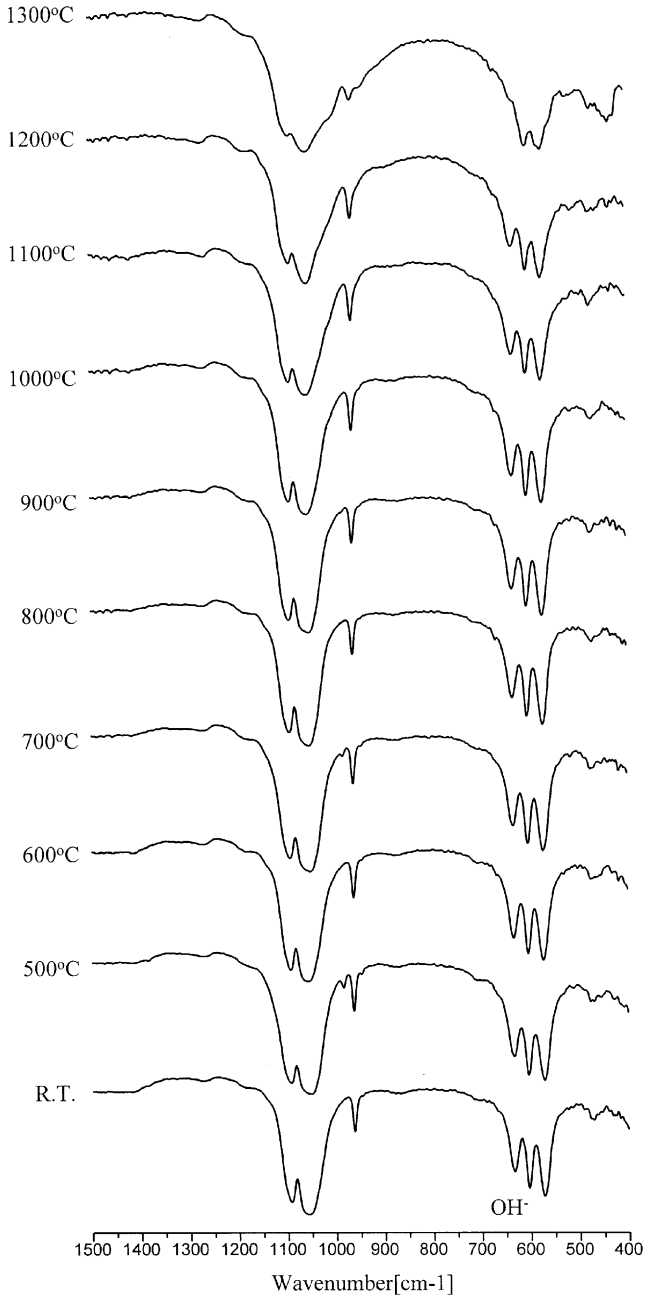

Fig. 4. FTIR spectra of CBB heated from room temperature to 1300°C.

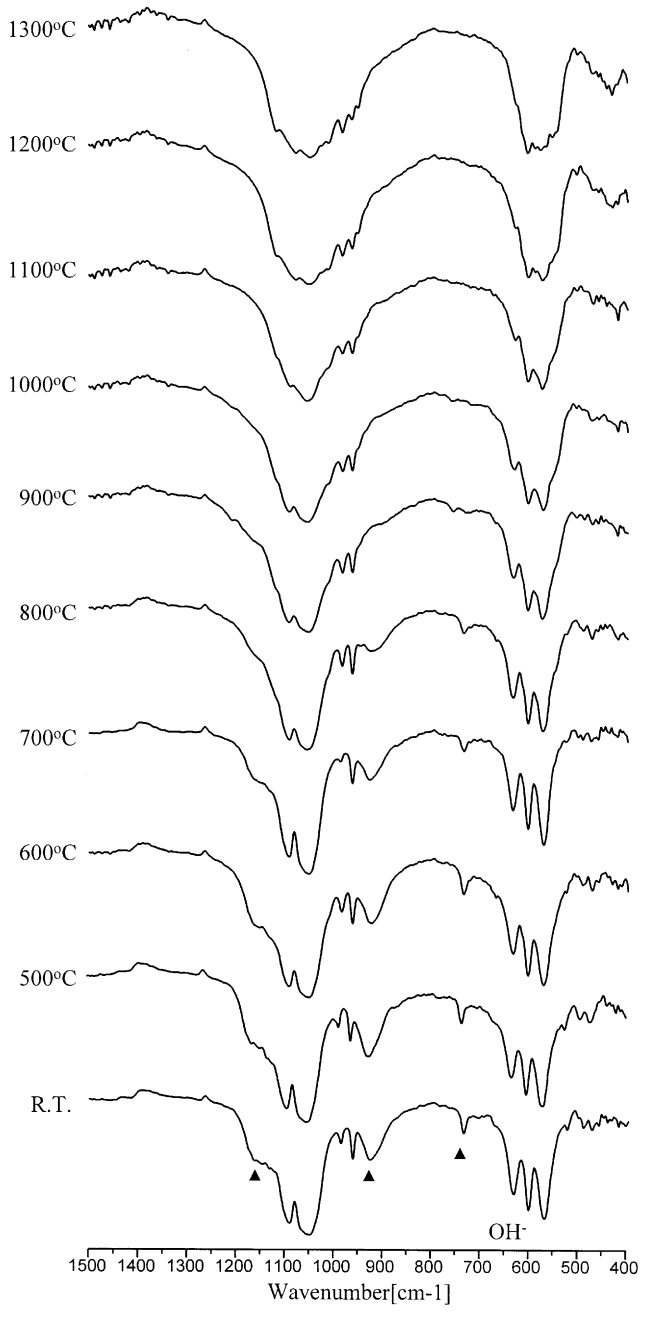

Fig. 5. FTIR spectra of CBB soaked in 0.05 M NP solution and heated from room temperature to 1300°C (▲: bands of NP).

the attention of researchers. It is known that stoichiometric HAP releases its OH^- ions and gradually transforms to oxyhydroxyapatite (OHAP, $Ca_{10}(PO_4)_6(OH)_{2-2X}O_X$) at temperatures up to 800°C [16]:

$$Ca_{10}(PO_4)_6(OH)_2 \rightarrow Ca_{10}(PO_4)_6(OH)_{2-2X}O_X + H_2O \quad (1)$$

When OHAP is heated at high temperature, it will decompose into tricalcium phosphate and tetracalcium phosphate (TTCP, $Ca_4P_2O_9$), which could be described as follows [17]:

$$Ca_{10}(PO_4)_6(OH)_2 \rightarrow 2Ca_3(PO_4)_2 + Ca_4P_2O_9 + H_2O \quad (2)$$

The decomposition temperature of HAP has been reported to mainly depend on the atmosphere of heating. If performed under vacuum, HAP loses its OH^- ions and decomposes into αTCP and TTCP around 1125°C. If HAP is heated in a H_2O stream, the decomposition

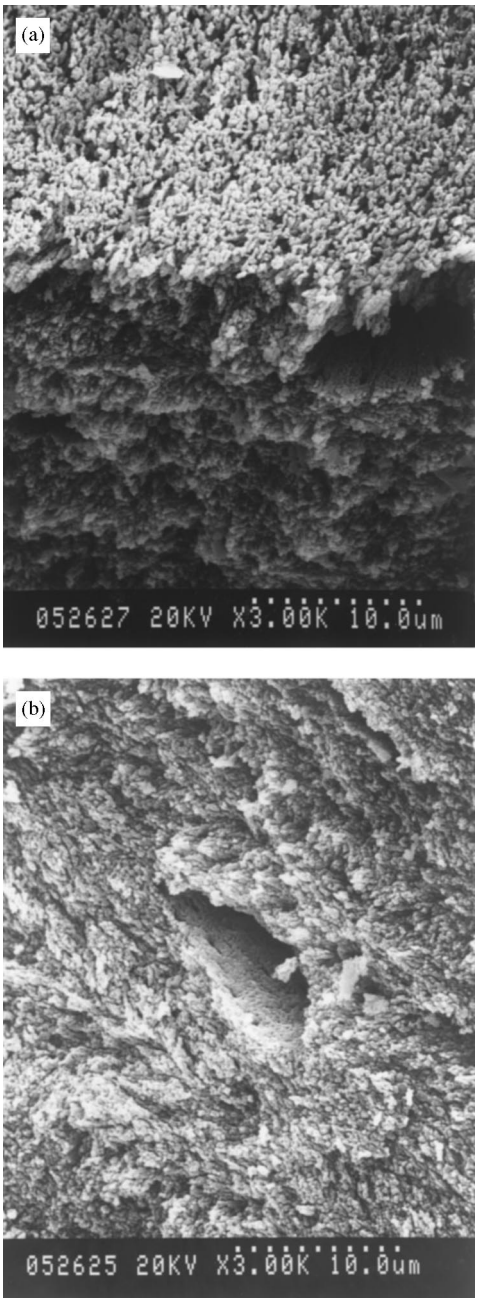

Fig. 6. The fracture surface of (a) CBB and (b) CBB soaked in 0.05 M NP solution for 24 h.

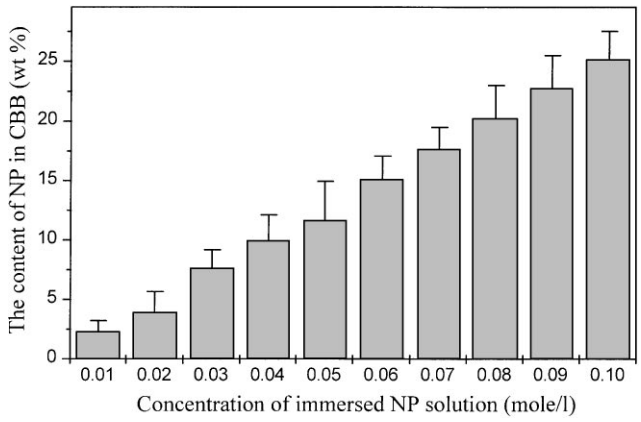

Fig. 7. Weight change of CBB block after being soaked in different concentrations of NP solution.

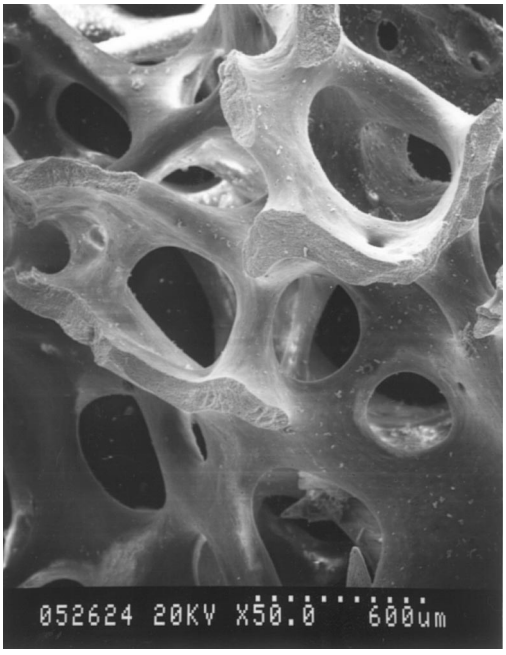

Fig. 8. SEM micrograph of the CBB soaked in 0.03 M NP solution and heated at 1300°C.

temperature of HAP will be raised up to 1400°C [13, 14]. In addition, the functional groups of HAP is also an important determinant factor for the decomposition temperature of HAP. Non-stoichiometric HAP, such as deficient HAP (d-HAP, $Ca_{10-x}(HPO_4)_x(PO_4)_{6-x}(OH)_{2-x}$) has the same crystal structure as HAP, but its decomposition temperature is lower than HAP. Since the HPO_4^{2-} ions of d-HAP are condensed into $P_2O_7^{4-}$ ($2HPO_4^{2-} \rightarrow P_2O_7^{4-} + H_2O$) in the temperature of 250°C to 550°C, $P_2O_7^{4-}$ will then react with the OH^- ions of d-HAP as the following formula: $P_2O_7^{4-} + 2OH^- \rightarrow 2PO_4^{3-} + H_2O$. It will lead to d-HAP decomposed into βTCP and HAP around 650°C [18, 19].

Crystallographic investigations of the bone minerals have shown that, apart from the main fraction exhibiting the base structure of HAP (containing stoichiometric HAP and non-stoichiometric HAP), bone contained other crystalline substances such as octacalcium phosphate ($Ca_8H_2(PO_4)_6 \cdot 5H_2O$, OCP), brushite ($CaHPO_4 \cdot 2H_2O$, DCP) and tricalcium phosphate [2]. Fowler [20] has studied the pyrolysis reactions of octacalcium phosphate. He showed that OCP and DCP

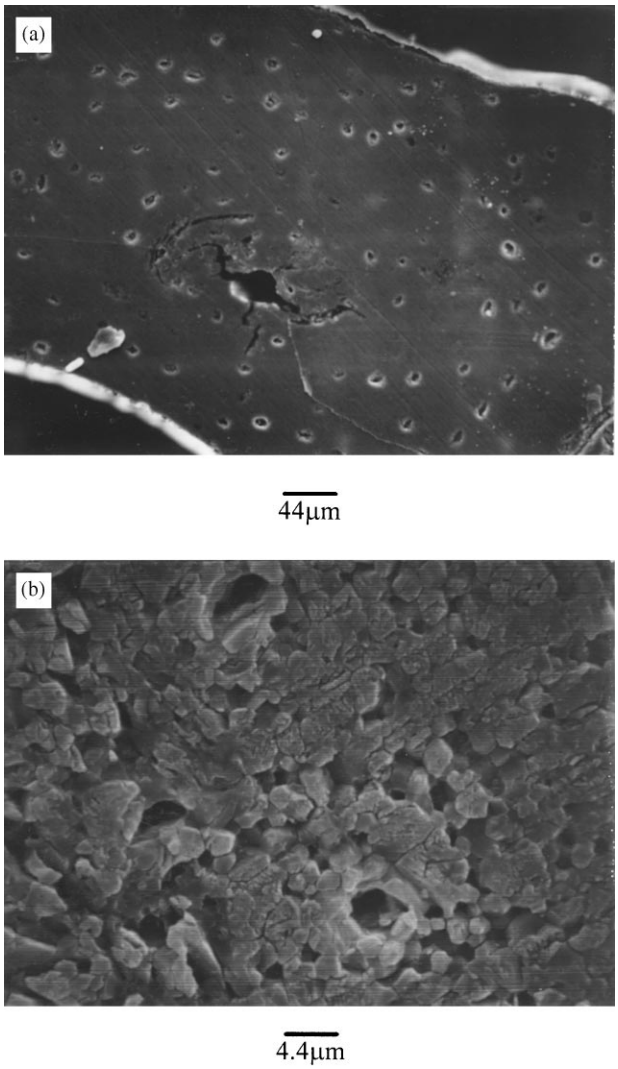

Fig. 9. SEM micrographs of trabecular section of CBB after being soaked in 0.03 M NP solution for 24 h and heated at 1300°C: (a) original magnification ×230; (b) original magnification ×2300.

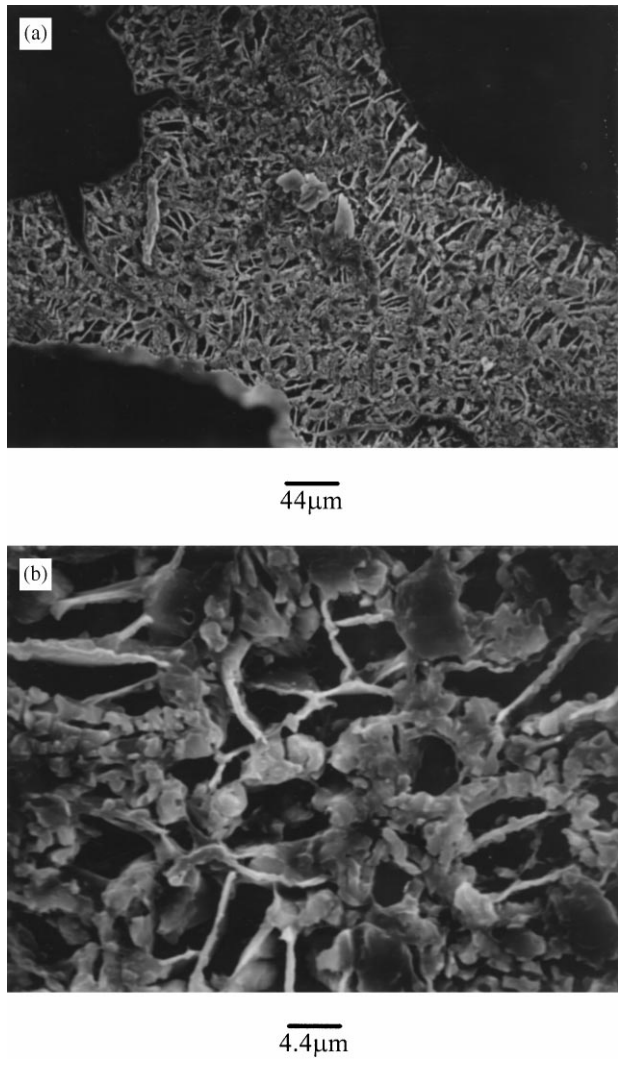

Fig. 10. SEM photographs of trabecular section of CBB after being soaked in 0.09 M NP solution for 24 h and heated at 1300°C: (a) original magnification ×230; (b) original magnification ×2300.

would be turned into calcium pyrophosphate ($Ca_2P_2O_7$) during heating, and calcium pyrophosphate could react with HAP of the bone to produce βTCP at a high temperature. Mittelmeier et al. [1, 2] heated the bovine cancellous bone and found that the sintered bovine bone and contained 93% of hydroxyapatite (natural bone contains 90%) and about 7% of tricalcium phosphate. In the present study, the sintered CBB exhibited a pure form of HAP crystalline structure. There were no significant differences in the XRD analysis when the heating temperature was raised from room temperature to 1300°C. No TCP characterized peaks or other crystalline phases have been traced in the CBB (Fig. 4). The results of FTIR analysis (Fig. 6) shows that CBB has a thermal behavior similar to the stoichiometric HAP, which gradually releases its OH^- ions and transforms to oxyapatite ($Ca_{10}(PO_4)_6O$) at high temperature.

In the previous study, d-HAP would decompose into HAP and βTCP around 650°C as follows:

$$Ca_{10-X}(HPO_4)_X(PO_4)_{6-X}(OH)_X \rightarrow 3XCa_3(PO_4)_2 + (1-X)Ca_{10}(PO_4)_6(OH)_2 + XH_2O \quad (3)$$

After d-HAP is added to NP, it would raise the concentration of $P_2O_7^{4-}$ ions in the system. The foreign $P_2O_7^{4-}$ ions coming from NP would further react with HAP, decomposed from d-HAP, to produce more βTCP in the system. In this study, NP doped to the CBB could also react with HAP to produce some of the chemical compounds containing PO_4^{3-} ions, i.e. βTCP. In Fig. 3, $NaCaPO_4$ could be traced in the XRD patterns around 600°C because of much more $P_2O_7^{4-}$ ions contained in

the system. The reaction of Eq. (4) might have happened in the system as follows:

$$3Ca_{10}(PO_4)_6(OH)_2 + 2Na_4P_2O_7 \rightarrow$$
$$8Ca_3(PO_4)_2 + 6NaCaPO_4 + Na_2O + 3H_2O \quad (4)$$

The results of FTIR (Fig. 5) showed that the bands of NP disappeared around 900°C. It reflected that the reaction of Eq. (4) might be completed at that temperature. When CBB with NP addition is heated over 900°C, characteristic peaks of βTCP increased with the heating temperature but both peaks of HAP and $NaCaPO_4$ showed a negative tendency with the heating temperature (Fig. 3). The authors speculated that HAP and $NaCaPO_4$ will further react to form βTCP as the following formula:

$$Ca_{10}(PO_4)_6(OH)_2 + 2NaCaPO_4 \rightarrow$$
$$4Ca_3(PO_4)_2 + 2NaPO_3 \quad (5)$$

Santos et al. [21] indicated that additions of Na_2O to the glass seems to be detrimental to the stability of HAP, giving rise to greater amounts of HAP transformed into TCP. Rey et al. [22] reported that, on heating to 1000°C, some of the sodium ions may enter into the apatite structure containing vacancies on OH^- sites leading to the imbalances in the Ca/P ratio of HAP, which could also lead to the appearance of βTCP. Kasgasnieni et al. [23] studied silicate-based glass matrices and found that the sodium ions could diffuse into the hydroxyapatite particle which then converted into $NaCaPO_4$ and led to HAP decomposition. It is known from Fig. 3 that the system will produce a large amount of $NaCaPO_4$ when heated up to 900°C. Sodium ions could be detrimental to the stability of HAP and then $NaCaPO_4$ might react with HAP to produce more βTCP in the system between 900 and 1300°C.

Summarizing from Eqs. (4) and (5) it is known that NP doped into CBB could react with the HAP of CBB to produce βTCP and $NaCaPO_4$ around 600°C. At high temperature, the $NaCaPO_4$ will further react with HAP to produce more βTCP in the system. Thus, while NP addition was lower in CBB such as in the condition of CBB soaked in NP solution with concentration in the range of 0.01–0.04 M, the product of the reaction of Eq. (4)—$NaCaPO_4$ would be used up in the reaction of Eq. (5) at high temperature to form a HAP/TCP biphasic crystalline structure. At higher NP additions such as the CBB soaked in NP solution with the concentration of 0.05–0.07 M, the residual $NaCaPO_4$ will be left in the system to form a HAP/TCP/$NaCaPO_4$ multiphasic crystalline structure. If CBB is soaked in an NP solution with a concentration over 0.08 M, HAP will completely react and form a TCP/$NaCaPO_4$ biphasic structure.

$NaCaPO_4$ has higher solubility which has been used as a phosphate fertilizer [24]. Kangasniemi et al. [23] suggested that $NaCaPO_4$ was as bioactive as HAP but exhibited a higher extent of dissolution in body environment. Ramselaar et al. [25] reported that $NaCaPO_4$ appeared to transform into an apatite containing carbonate, sodium and magnesium while it was inserted in tooth sockets of beagle dogs for six months. Thus, from the biological point of view $NaCaPO_4$ has similar biodegradable properties with TCP, if HAP ceramic contains $NaCaPO_4$, the high solubility of $NaCaPO_4$ could also improve the bioactivity of HAP in vivo. Additionally, $NaCaPO_4$ has higher solubility than TCP [26], we could develop a new bioresorbable ceramic which has a higher bioresorbability than TCP ceramic, i.e. TCP/$NaCaPO_4$ ceramic or $NaCaPO_4$ ceramic by heating CBB with high NP addition.

5. Conclusion

In the present study, the CBB exhibited a pure form of HAP characterized patterns, there were no other crystalline phases to be traced during heating. The thermal behavior of CBB was similar with stoichiometric HAP, which loses its OH^- ions and gradually transforms into oxyhydroxyapatite at high temperature. NP doped into CBB could react with HAP of calcined bone to produce βTCP and $NaCaPO_4$ around 600°C. At 900°C, NP addition would be used up and the $NaCaPO_4$ could further react with HAP to produce more βTCP in the system.

The crystalline phase composition of CBB could be changed by doping with different contents of NP in CBB and heated at high temperature. As the NP addition increases, the phase composition of CBB would gradually transform from stoichiometric HAP to HAP/TCP, HAP/TCP/$NaCaPO_4$ or TCP/$NaCaPO_4$. We could utilize this process to prepare different crystalline phase compositions with a natural bone structure.

References

[1] Urist MR, O'Connor BT, Burwell RG. Bone grafts, derivatives and substitutes. London: Butterworth-Heinemann, 1994.
[2] Katthagen BD. Bone regeneration with bone substitutes. Boca Raton, FL: CRC Press, 1983.
[3] Maatz R. A new method of bone maceration. J Bone Jt Surg 1957; 39A:153–66.
[4] Maatz R, Lenz W, Graf R. Spongiosa test of bone grafts for transplantation. J Bone Jt Surg 1954;36A:721–31.
[5] Salama R. Xenogeneic bone grafting in humans. Clin Orthop 1983;174:113–21.
[6] Salama R, Gazit E. The antigenicity of Kiel bone in the human host. J Bone Jt Surg 1978;60B:262–5.
[7] Aoki H. Medical application of hydroxyapatite. Ishiyaku Euro America Inc., Tokyo, St. Louis: Takayama Press, 1994.
[8] Jarcho M. Calcium phosphate ceramics as hard tissue prosthetics. Clin Orthop Relat Res 1981;157:259–78.

[9] de Groot K. Bioceramics of calcium phosphate. Boca Raton, FL: CRC Press, 1983.
[10] Kohri M, Miki K, Waite DE, Nakajima H, Okabe T. In vivo stability of biphasic calcium phosphate ceramics. Biomaterials 1993;14:299–304.
[11] Frayssinet P, Trouillet JL, Rouquet N, Azimus E, Autefage A. Osseointegration of macroporous calcium phosphate ceramics having a different chemical composition. Biomaterials 1993; 14:423–9.
[12] Nery EB, LeGeros RZ, Lynch KL, Lee K. Tissue response to biphasic calcium phosphate ceramic with different ratios of HA/βTCP in periodontal osseous defects. J Periodontol 1992; 63:729–35.
[13] Locardi B, Pazzaglia UE, Gabbi C, Profilo B. Thermal behaviour of hydroxyapatite intended for medical applications. Biomaterials 1993;14:437–441.
[14] Ellies LG, Nelson DG, Featherstone JD. Crystallographic changes in calcium phosphates during plasma-spraying. Biomaterials 1992;13:313–6.
[15] Chen J, Tong W, Yang C, Feng J, Zhang X. Effect of atmosphere on phase transformation in plasma-sprayed hydroxyapatite coatings during heat treatment. J Biomed Mater Res 1997;34:15–20.
[16] Trombe JC, Montel G. Some features of the incorporation of oxygen in different oxidation states in the apatitic lattice—II. J Inorg Nucl Chem 1977;40:23–6.
[17] Jiming Z, Zhang X, Xingdong C, Jiyong Z, Shaoxian, de Groot K. High temperature characteristics of synthetic hydroxyapatite. J Mater Sci: Mater Med 1993;4:83–5.
[18] Ishikawa K, Ducheyne P, Radin S. Determination of the Ca/P ratio in calcium-deficient hydroxyapatite using X-ray diffraction analysis. J Mater Sci: Mater Med 1993;4:165–8.
[19] Yubao L, Klein CPAT, de Wijn J, Van de Meer S. Preparation and characterization of nanograde osteoapatite-like rod crystals. J Mater Sci: Mater Med 1994;5:252–5.
[20] Fowler BO, Moreno EC, Brown WE. Infra-red spectra of hydroxyapatite, octacalcium phosphate and pyrolysed octacalcium phosphate. Arch Oral Biol 1966;11:477–92.
[21] Santos JD, Knowles JC, Reis RL, Monteiro FJ, Hastings GW. Microstructural characterization of glass-reinforced hydroxyapatite composites. Biomaterials 1994;15:5–10.
[22] Rey C, Trombe JC, Montel G. Retention of molecular oxygen by the lattice of certain alkaline earth apatites. C R Acad Sci Ser C 1973;276:1385–8.
[23] Kangasniemi I, de Groot K, Wolke J, Andersson O, Luklinska Z, Becht JGM, Lakkisto M, Yli-Urpo A. The stability of hydroxyapatite in an optimized bioactive glass matrix at sintering temperature. J Mater Sci: Mater Med 1991;2:133–7.
[24] Ando J, Matsuno S, $Ca_3(PO_4)_2$–$CaNaPO_4$ system. Bull Chem Soc Jpn 1968;41:342–7.
[25] Ramselaar MMA, van Mullem PJ, Kalk W, Driessens FCM, de Wijn JR, Stols ALH. In vivo reactions to particulate rehenanite and particulate hydroxyapatite after implantation in tooth sockets. J Mater Sci-Mater Med 1993;4:311–7.
[26] Berger G, Gildenhaar R, Ploska U. Rapid resorbable, glassy crystalline materials on the basic of calcium alkali orthophosphates. Biomaterials 1995;16:1241–8.